Bacterial Iron Transport: ^{1}H NMR Determination of the Three-Dimensional Structure of the Gallium Complex of Pyoverdin G4R, the Peptidic Siderophore of *Pseudomonas putida* G4R[†,‡]

R. Andrew Atkinson,[§,||] Abdel Latif M. Salah El Din,[⊥] Bruno Kieffer,[§] Jean-François Lefèvre,[§] and Mohamed A. Abdallah*[,⊥]

Laboratoire de Chimie Microbienne, Associé au CNRS, and UPR 9003 du CNRS, Ecole Supérieure de Biotechnologie de Strasbourg, Bd. Sébastien Brant, 67400 Illkirch, France

Received May 20, 1998; Revised Manuscript Received August 24, 1998

ABSTRACT: Among the fluorescent *Pseudomonas* species, *Pseudomonas putida* is a rare case of a nitrogen-fixing bacterium that transforms nitrogen into ammonia. When grown under iron-deficient conditions, it produces two major pyoverdins: pyoverdin G4R and pyoverdin G4RA. Their primary structures have been established using FAB-MS and one- and two-dimensional ^{15}N, ^{13}C, and ^{1}H NMR on both the unlabeled and ^{15}N-labeled compounds [Salah El Din, A. L. M., et al. (1997) *Tetrahedron 53*, 12539−12552]. The two pyoverdins have a common chromophore derived from 2,3-diamino-6,7-dihydroxyquinoline. The chromophore is bound to the linear heptapeptide L-Asp-L-Orn-D-*β-threo*-OHAsp-L-Dab-Gly-L-Ser-L-*cyclo*-OHOrn. Circular dichroism spectra suggest that the absolute configuration of the metal complex is Δ. The three-dimensional structure in solution of pyoverdin G4R−Ga(III) was determined after interpretation of two-dimensional ^{1}H NMR spectra recorded at 283 and 303 K. The complex is tightly defined with a compact structure with a Δ absolute configuration. The site of complexation of the metal ion is found to be located on the surface of the molecule, showing that the ion can be released without large conformational changes, while the polar groups of the peptide chain, which may be responsible for the recognition of the receptor, are placed on the opposite side of the overall shape. The three-dimensional structure of pyoverdin G4R−Ga(III) is compared with those of other pyoverdins, and the role of the structure in iron uptake is discussed.

Iron is an essential element in many microorganisms. It catalyzes electron transfer in reactions as critical and as different as those occurring in the transport or the storage of oxygen (hemoglobin and myoglobin) and in the metabolism of hydrogen (hydrogenases), oxygen (peroxidase and catalase), or nitrogen (nitrogenases). It is also present in a number of flavoproteins and sulfur proteins (*2*). The redox potential of the Fe(III)−Fe(II) system can vary from −490 (in the case of sulfur proteins) to 385 mV (for the cytochromes). This is why proteins such as ferredoxins can catalyze the transfer of electrons, required for the energetic metabolism of anaerobic bacteria, at very low potentials. In contrast, iron porphyrins, such as cytochrome oxidase, which probably control all aerobic life, have much higher redox potentials (*3*).

Despite the abundance of iron in the earth's crust (5%), its availability is severely limited by the very high insolubility of iron(III) at physiological pH. In the presence of oxygen, iron(II) is rapidly oxidized to iron(III) which precipitates as a polymeric oxyhydroxide. The solubility product of ferric hydroxide is extremely low (10^{-38} M[4]) such that, at physiological pH, the concentration of free iron(III) is less than 10^{-17} M. This value is far too low to allow the growth of aerobic microorganisms (*4*).

Iron metabolism in microorganisms relies upon the biosynthesis of low-molecular mass compounds (300−2000 Da) called siderophores (*5*). These molecules are generally secreted into the culture medium where they chelate iron(III) very strongly, thus solubilizing it. Following chelation, the iron(III) is transported into the cells using an ATP-dependent, high-affinity transport system (*6*). In Gram-negative bacteria, the siderophore−iron(III) complex crosses the outer membrane by means of iron-regulated outer-membrane proteins (IROMPs) (*6*−*11*). The complexes are probably transferred into the periplasmic space where a permease facilitates their passage through the cytoplasmic membrane. Iron is released into the cytoplasm by a reductive process (*12*). Siderophore−iron(II) complexes appear to be much less stable, in general, than the corresponding iron(III) complexes, and it is not surprising that iron(II) can be released for insertion, as such or as iron(III), into the sites of iron proteins present in the cytoplasm.

[†] R.A.A. gratefully acknowledges receipt of an Eli Lilly postdoctoral fellowship, and we thank the Ministère des Affaires Etrangères for a grant for one of us (A.L.M.S.E.D.) and the Centre National de la Recherche Scientifique for financial support (ARI Chimie-Biologie).

[‡] NMR data are deposited at the BioMagResBank under accession numbers 4164 [pyoverdin G4R−Ga(III) (structures and NMR parameters)] and 4169 [pyoverdin G4R free ligand (NMR parameters)].

* To whom correspondence should be addressed. Fax: (+33) (0)3 88 65 52 34. E-mail: abdallah@chimie.u-strasbg.fr.

[§] UPR 9003 du CNRS, Ecole Supérieure de Biotechnologie de Strasbourg.

[||] Present address: National Institute for Medical Research, The Ridgeway, Mill Hill, London NW7 1AA, U.K.

[⊥] Laboratoire de Chimie Microbienne, Associé au CNRS, Ecole Supérieure de Biotechnologie de Strasbourg.

10.1021/bi981194m CCC: $15.00
Published on Web 10/20/1998

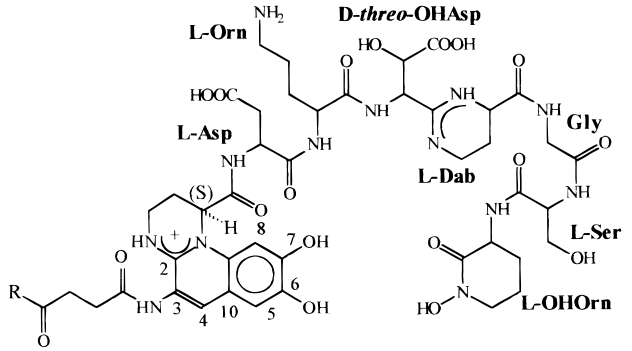

FIGURE 1: Primary structure of pyoverdin G4R (R = NH_2) and G4RA (R = OH).

When fluorescent *Pseudomonas* are cultivated under iron-deficient conditions, they secrete a number of yellow-green, water-soluble, fluorescent siderophores called pyoverdins. These substances are chromopeptides with a molecular mass of 1000−1500 Da (*13*). They possess a common chromophore derived from 2,3-diamino-6,7-dihydroxyquinoline bound to a peptidic moiety of 6−12 amino acids. This peptide is identical for all pyoverdins produced by a given strain but differs from strain to strain. The amino acids may be neutral (glycine, alanine, serine, homoserine, glutamine, and citrulline), acidic (β-hydroxyaspartic acid, aspartic acid, and glutamic acid), or basic (N^{δ}-hydroxyornithine, ornithine, lysine, 2,4-diaminobutyric acid, and arginine) and may occur in either configuration. On the other hand, the chromophore has the same configuration (*S*) for all pyoverdins investigated so far. For a given strain, the pyoverdins differ only in the acyl substituent bound to the amino group on C3 of the chromophore (see Figure 1), which may be derived from succinic acid, malic acid, or α-ketoglutaric acid (*13*), or from many other diacids in the Krebs cycle (*14*).

Pyoverdins have a high affinity for ferric iron (*15*, *16*), forming very stable octahedral complexes. The three functional bidentate groups involved in the complexation are the catechol function of the chromophore and either two hydroxamate functions (N^{δ}-acyl, N^{δ}-hydroxyornithines) or one hydroxy acid (generally D-β-*threo*-hydroxyaspartic acid) and one hydroxamate (generally *cyclo*-N^{δ}-hydroxyornithine), present in the peptide moiety.

The diversity of these siderophores reveals large differences in their primary structures, not only in the nature of the amino acids but also in the manner in which they are connected. The peptidic moiety may be linear, partly cyclic (*17*−*20*), or fully cyclic (*21*). These great structural differences render the problem of characterization of the pyoverdins highly complex such that a combination of powerful techniques including two-dimensional NMR and FAB-MS[1] is required, to compensate for the lack of diffracting crystals (*13*). They also explain the high specificity of these siderophores for the strains which generate them, a specificity achieved in the recognition step at the outer-membrane receptor proteins. At present, nothing is known about the nature of the amino acids or the steric features of the peptide chain that govern the interactions of pyoverdins with their outer-membrane receptors.

Although there is a number of primary structures of pyoverdins reported, there are only two examples in the literature of the three-dimensional structures of pyoverdins. The first is that of the pseudobactin B10−iron(III) complex determined by X-ray crystallography, establishing a Λ absolute configuration for the iron(III) complex (*22*); the second is the NMR solution structure of pyoverdin GM-II−Ga(III) which shows a different isomer but retains a Λ absolute configuration (*23*).

Among the fluorescent *Pseudomonas* species, *Pseudomonas putida* G4R is a rare case of a nitrogen-fixing bacterium that transforms nitrogen into ammonia. From the cultures of this bacterium grown under iron-deficient conditions, two major pyoverdins, pyoverdin G4RA and pyoverdin G4R, were isolated, and their primary structure (Figure 1) was elucidated using FAB-MS and two-dimensional NMR on both unlabeled and ^{15}N-labeled molecules (*1*). They are chromopeptides possessing the linear heptapeptide L-Asp-L-Orn-D-β-*threo*-OHAsp-L-Dab-Gly-L-Ser-L-*cyclo*-OHOrn, bearing a novel, natural amino acid that results from the condensation of D-β-*threo*-hydroxyaspartic acid with L-2,4-diaminobutyric acid. The precise role played by this additional tetrahydropyrimidine ring, located in the peptide chain, in pyoverdin-mediated iron transport was not immediately clear.

In this paper, we describe the three-dimensional structure of the pyoverdin G4R−Ga(III) complex, determined by NMR spectroscopy, and analyze the features of the structure responsible for iron complexation and those that may govern receptor binding. The three-dimensional structure of pyoverdin G4R−Ga(III) is compared with those of other pyoverdins and siderophores.

EXPERIMENTAL PROCEDURES

Sample Preparations. The strain, culture medium, isolation and purification of the pyoverdins as free ligands, and preparation of the pyoverdin G4R−Fe(III) complex were as reported by Salah El Din et al. (*1*). Ferric pseudobactin B10 was prepared from pseudobactin isolated and purified from cultures of *Pseudomonas* B10 according to Teintze et al. (*22*).

Pyoverdin G4R (or G4RA) pure free ligand (25 mg) was dissolved in 2 mL of distilled water and the mixture treated with 5 equiv of 0.1 M gallium(III) nitrate (1.15 mL). The solution was kept for 1 h at room temperature, and applied on a CM-Sephadex column (1.0 cm × 12 cm), eluted first with 0.05 M pyridine/acetic acid buffer (pH 5.0, 60 mL), and then with a linear gradient of the same buffer (0.05 to 0.25 M, 2 × 100 mL). The yield of pure complex was 20 mg.

UV−*Visible Spectroscopy*. Spectra were acquired on a Kontron Uvikon 930 spectrophotometer (Kontron Intruments,

[1] The terms "pyoverdin G4R" and "pyoverdin G4RA" refer to uncomplexed, ^{15}N-labeled (or unlabeled) succinamide (G4R) and succinate (G4RA) samples, respectively. The suffixes −Fe(III) and −Ga(III) denote the complexed forms. Succinate or succinamide groups are referred to as Suc, and the chromophore (2,3-diamino-6,7-dihydroxyquinoline) is referred to as Chr. For the peptide chain, the following abbreviations are used: Asp1, L-aspartic acid; Orn2, L-ornithine; OHAsp3, D-β-*threo*-hydroxyaspartic acid; Dab4, L-2,4-diaminobutyric acid (in its cyclized carboxytetrahydropyrimidine form); Gly5, glycine; Ser6, L-serine; OHOrn7, L-*cyclo*-N^{δ}-hydroxyornithine. Formyl is referred to as Fo. Other abbreviations: CD, circular dichroism; COSY, two-dimensional correlated spectroscopy; DQF-COSY, double-quantum filtered two-dimensional correlated spectroscopy; FAB-MS, fast atom bombardment mass spectroscopy; HOHAHA, homonuclear Hartmann−Hahn spectroscopy; NOESY, nuclear Overhauser enhancement spectroscopy; ROESY, rotating frame Overhauser enhancement spectroscopy; rmsd, root-mean-square deviation.

Saint Quentin en Yvelines, France). The solvents were 0.1 M acetate buffer (pH 4.0 and 5.0) and 0.2 M phosphate buffer (pH 7.2).

The extinction coefficient of ferric pyoverdin G4R at its absorption maximum was calculated from the absorbance of an aqueous solution whose iron concentration was measured by atomic absorption spectroscopy using either a Techtron 1200 or a Jobin-Yvon ICP 2500 instrument (*24*). The extinction coefficient of pyoverdin G4R was deduced after titration of pyoverdin G4R free ligand at a given pH with a 10^{-2} M ferric chloride solution. The extinction coefficient of pyoverdin G4R−Ga(III) at its absorption maximum was deduced after titration of pyoverdin G4R free ligand with a 10^{-2} M gallium nitrate solution.

Mass Spectrometry. Mass sprectrometry was performed on an Autospec 6F instrument equipped with an electrospray source (Micromass, Altrincham, U.K.). The mobile phase was a mixture of H_2O/methanol (1:1) acidified with 1% acetic acid, at a flow rate of 10 μL/min. The sampling cone was at 50 eV, and the temperature of the source 80 °C. The samples were dissolved in a mixture of H_2O/methanol (1:1) acidified with 1% acetic acid and injected using a rheodyn injector fitted with a 10 μL loop.

Circular Dichroism Measurements. All spectra were measured on a Jobin-Yvon CD6 instrument, at 25 °C, using 1 cm optical pathway quartz cells (Hellma). Data points were recorded between 600 and 300 nm, every 1 nm, with a time constant of 1 s. The results are the average of three repetitive scans, corrected for solvent contribution. The solvents were 0.1 M acetate buffer (pH 4.0 and 5.0) and 0.2 M phosphate buffer (pH 7.2). The concentration of the pyoverdin used in the measurements was 4.5×10^{-5} M, as determined by spectrophotometry.

^{1}H NMR Spectroscopy. A similar set of ^{1}H NMR experiments was carried out for each of the following pyoverdin samples dissolved in H_2O/1% [$^2H_{10}$]-*tert*-butyl alcohol (CEA, Saclay, France): unlabeled pyoverdin G4RA−Ga(III), ^{15}N-labeled G4R, and ^{15}N-labeled G4R−Ga(III). All NMR measurements were taken at 283 and 303 K and at 500 MHz (^{1}H frequency) on a Bruker AMX 500 spectrometer.

Standard two-dimensional ^{1}H scalar and dipolar coupling experiments were carried out in the phase-sensitive mode, using time-proportional phase incrementation (TPPI) (*25*), with a spectral width of 6024 or 6579 Hz in both dimensions and a relaxation delay of 3 s. COSY (*26*) and DQF-COSY (*27*) spectra were recorded with presaturation of the water signal during the relaxation delay; HOHAHA (*28*, *29*), NOESY (*30*), and ROESY (*31*) spectra were recorded with suppression of the water signal using a WATERGATE sequence (*32*) prior to acquisition. For the HOHAHA experiment, a spin-locking rotating frame field strength of ca. 8.5 kHz and a mixing time of 80 ms were used; NOESY spectra were acquired with mixing times between 25 and 400 ms, and ROESY spectra were recorded with a rotating frame field strength of ca. 2.5 kHz and a mixing time of 80 ms. Pulse sequences for experiments with ^{15}N-labeled samples were modified by the addition of 180° refocusing ^{15}N pulses at the center of the t_1 evolution period and GARP decoupling (*33*) during acquisition. In most cases, 32 transients of 2K data points were acquired for each of the 512 t_1 increments.

Spectra were processed using the manufacturer's software, UXNMR, and using Felix (version 2.1, Biosym Technologies, San Diego, CA). In each dimension, COSY data were multiplied by an unshifted sine bell function and HOHAHA, NOESY, and ROESY data by a 90°-shifted sine bell function prior to zero-filling once and Fourier transformation.

HN Exchange. Hydrogen−deuterium exchange was investigated simply by recording a one-dimensional ^{1}H spectra at 283 K, immediately following dissolution in D_2O.

Coupling Constants and Dihedral Angles. Coupling constants ($^3J_{HN-H\alpha}$) were measured on one-dimensional spectra with 8K data points acquired and zero-filled to 16K points. Possible values of ϕ angles were calculated from $^3J_{HN-H\alpha}$ values using the Karplus relationship (*34*) and the parameters of Pardi et al. (*35*). ϕ angles derived from $^3J_{HN-H\alpha}$ coupling constants were not introduced as constraints during the structural calculations but used as a check on calculated structures.

Stereospecific Assignments. $^3J_{H\alpha-H\beta}$ coupling constants were classified as large or small, on the basis of the pattern of splitting of the Hα−Hβ cross-peak in the COSY spectrum, and, with the intensities of HN−Hβ and Hα−Hβ ROE cross-peaks, used to assign prochiral Hβ resonances stereospecifically, where possible (*36*).

Distance Constraints. The intensities of cross-peaks in ROESY spectra of pyoverdins G4RA−Ga(III) and G4R−Ga(III) were measured. Data from the unlabeled pyoverdin G4RA−Ga(III) sample were used in the following experiment. An initial calibration based on the intensity of the cross-peak between the aromatic protons of the chromophore, Chr H4 and Chr H5, was tightened such that the distances corresponding to HN_i−Hα_i cross-peaks satisfied the permitted range. The upper limit for each constraint was set to 15% greater than the calculated distance, for cross-peaks involving HN resonances and aromatic resonances. A larger tolerance (20% of the calculated distance) was used in fixing the upper bound for constraints between aliphatic protons, since many of these cross-peaks are partially overlapped with others. Lower bounds were set to zero for all constraints derived from spectra.

Structure Calculations. All calculations were carried out on IBM RS/6000 machines, using standard protocols (sa, refine, accept) in X-PLOR 3.1 (*37*). The standard topology and parameter files (topallhdg.pro and parallhdg.pro) were modified to allow definition of the chromophore and the nonstandard residues of the pyoverdin. Nonbonded parameters for the Ga(III) ion were set to the same values used for iron atoms in standard X-PLOR parameter sets (the radii of the two ions are similar). Analysis of sets of calculated structures was carried out using in-house X-PLOR scripts and FORTRAN programs. Structures were visualized using Insight (Biosym Technologies).

A total of 119 distance constraints, derived from 80 ms ROESY spectra, were used as upper limits on interproton distances, with no lower limit specified, and applying standard pseudoatom corrections where required (*38*). Of these constraints, 78 were intraresidue, 32 sequential, and 9 other. Where cross-peaks to both resonances of unresolved prochiral pairs were observed, both constraints were set to the longer distance with no correction. Coordination of the Ga(III) ion was defined solely by distance constraints between each of six oxygen atoms (Chr O6, Chr O7,

OHAsp3 OG1, OHAsp3 OD1, OHOrn7 O, and OHOrn7 OE) and the metal ion, with no imposition of coordination geometry; distances (d_{Ga-O}) were set to cover the range of values found in crystallographic studies of siderophores (*22*): 2.04 ± 0.04 Å, except for $d_{Ga-OHOrn7OE}$, which was set to 1.98 ± 0.04 Å. A force constant of 50.0 kcal mol^{-1} Å^{-2} was applied to all distance constraints.

Initial calculations were carried out with no stereospecific assignments and no dihedral angle constraints. Resulting structures were analyzed for consistency with stereospecific assignments and dihedral angles derived from spectra. The distance constraint list was revised to include stereospecific assignments, and a set of 100 structures was generated with the modified set of constraints. In a further series of calculations, all 16 possible octahedral configurations of the three bidentate ligands around the metal ion were explored; distances between pairs of coordinating oxygen atoms on adjacent vertexes of the octahedron were set to $d_{O-O} = 2.83 \pm 0.3$ Å, and one improper angle was defined to set the chirality of the coordination sphere. For each of the 16 configurations, a set of five structures were calculated and the energies of each family analyzed.

RESULTS

Characterization of the Pyoverdin G4R−Ga(III) Complex. The UV−visible spectrum of the pyoverdin G4R−Ga(III) complex exhibits a maximum at 408 nm ($\epsilon_{408} = 21\,500$ M^{-1} cm^{-1}) at pH 5.0. Blue fluorescence is observed upon excitation of the solution at 364 nm in contrast to the nonfluorescent iron complex. Magnetic electrospray mass spectrometry performed on the ^{15}N-labeled pyoverdin G4R−Ga(III) complex gave signals at 1153 and 1155 mu, characteristic of the two isotopes of gallium, ^{69}Ga and ^{71}Ga, and confirming the 1:1 stoichiometry of the complex.

Circular Dichroism. The solution structure of pyoverdins is characterized by the absolute configuration of the coordination sphere, the configuration of the asymmetric carbon atom C11 bound to the chromophore, and the amino acids and finally the conformation of the peptide chain. Sixteen possible octahedral configurations of the three bidentate ligands around the metal ion, namely eight Λ and eight Δ, have to be considered a priori, although many of them could be generally excluded for steric hindrance reasons. The absolute configuration of the sphere of coordination can be established by CD spectroscopy.

It has been observed that the Λ coordination isomers of triacetylfusarinine observed in the crystalline state isomerized upon dissolution into the predominant Δ isomers (*39*). In the crystalline form, ferric pseudobactin occurs as a Λ coordination isomer, and the CD bands due to the charge transfer absorption are qualitatively similar to those presented by triacetylfusarinine C. Therefore, one cannot exclude a priori the occurrence of an equilibrium between the Λ and Δ coordination isomers in solution.

The circular dichroism spectrum of pyoverdin G4R as a free ligand is highly pH-sensitive. At pH 4.0, positive Cotton effects are observed at 365 and 380 nm. At pH 5.0, the Cotton effects remain positive, showing a decrease in their intensities, while at pH 7.2, the maxima are shifted to higher wavelengths (380 and 400 nm). These results are comparable to those reported for pseudobactin B10 (*22*) and other pyoverdins (*13*, *14*, *40*) and indicate that the configuration of the asymmetric carbon atom C11 bound to the chromophore is *S*.

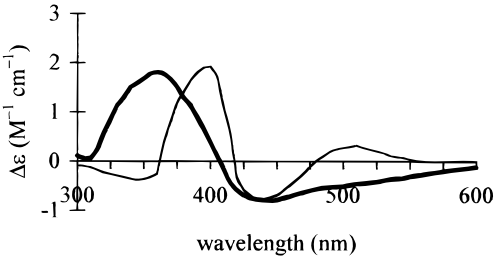

FIGURE 2: Circular dichroism spectra of ferric pseudobactin (thin line) and pyoverdin G4R−Fe(III) (thick line).

The circular dichroism spectrum of the pyoverdin G4RA−Fe(III) complex has been measured at three pH values, namely 4.0, 5.0, and 7.2. No difference was found between the three spectra which show the same positive Cotton effect between 310 and 405 nm with a maximum at 360 nm ($\Delta\epsilon = 1.7$ M^{-1} cm^{-1}) and the same two negative Cotton effects between 405 and 600 nm with a minimum at 440 nm ($\Delta\epsilon = -0.8$ M^{-1} cm^{-1}) and a shoulder at 540 nm ($\Delta\epsilon = -0.3$ M^{-1} cm^{-1}) (*1*). It exhibits some similarities with the spectrum of ferric pseudobactin, showing a comparable intense positive Cotton effect in the 310−405 nm range (ferric pseudobactin has a maximum at 400 nm) and the same negative Cotton effect at 440 nm. It differs at higher wavelengths; the weak negative Cotton effect shown by pyoverdin G4R−Fe(III) above 475 nm (Figure 2) compared to the weak positive Cotton effect shown by ferric pseudobactin B10 (*22*) and pyoverdin GMII−Fe(III) (*23*) in the same range suggests that pyoverdin G4R−Fe(III) is predominantly in a Δ absolute configuration.

Assignment of ^{1}H Resonances. All resonances in the ^{1}H spectra of each of the samples could be assigned in a straightforward manner by applying the sequential assignment method pioneered by Wüthrich (*41*) to a combination of COSY, HOHAHA, NOESY, and ROESY spectra, to confirm the unique spin systems of the pyoverdin G4R structure.

Assignments of pyoverdin G4R free ligand (Table 1) are close to those published previously for pyoverdin G4RA (*1*). Similarly, comparison of the assignments (at 283 K) of pyoverdin G4RA−Ga(III) (data not shown) with those of pyoverdin G4R−Ga(III) (Table 1) shows no major changes in chemical shifts between these two complexed samples. Only the Suc Hα and H*β* and Chr H4, H5, and H8 resonances are shifted slightly, and the Suc H*δ* amide protons appear for the latter sample at 7.59 and 6.82 ppm. A weak set of secondary resonances could be observed for Chr H11, H12, and H13 and OHAsp3 HN and Ser6 HN, in HOHAHA spectra of pyoverdin G4R−Ga(III). Spectra acquired at 303 K showed that these do not result from a conformational equilibrium, but probably from small amounts of pyoverdin G4RA arising from the slow hydrolysis of pyoverdin G4R (*19*).

Differences in ^{1}H chemical shifts (at 283 K) between complexed pyoverdin G4R−Ga(III) and uncomplexed pyoverdin G4R are, however, considerable (Table 1 and Figure 3). The dispersion of chemical shifts of the HN resonances over 2.5 ppm in the spectra of the complex, whereas in the

Table 1: Assignment of ^{1}H Resonances for Pyoverdin G4R and Pyoverdin G4R−Ga(III) at 283 K in H_2O/1% [$^2H_{10}$]-*tert*-Butyl Alcohol[a]

	chemical shift (ppm)						
	HN	Hα	Hβ	Hγ	Hδ	Hε	Δδ (ppb K^{-1})
Suc	**9.70**	**2.66**	**2.59**	−	**7.59, 6.82**		**−9.0**
	−	2.68	2.59	−	−		−
Asp1	**8.70**	**4.63**	**2.83, 2.63**				**−9.5**
	8.85	4.38	2.73, 2.63				−7.0
Orn2	**8.52**	**4.16**	**1.81, 1.72**	**1.65**	**3.04, 2.92**	**7.66**	**−9.5**
	8.37	4.15	1.58, 1.54	1.46	2.83	−	−6.0
OHAsp3	**9.22**	**5.16**	**4.78**				**−4.0**
	8.82	5.06	4.42				−8.0
Dab4	**9.56**	**4.19**	**1.89, 1.81**	**2.91, 1.71**	**8.12**		**−4.0**
	−	4.16	2.03, 1.91	3.36, 3.02	−		−
Gly5	**10.44**	**4.63, 4.04**					**−4.5**
	8.32	3.87					−4.5
Ser6	**8.30**	**4.28**	**3.79**				**−5.5**
	8.38	4.32	3.74				−7.0
OHOrn7	**8.45**	**4.68**	**2.06, 1.65**	**1.90, 1.84**	**3.47**		**−4.5**
	8.45	4.32	1.87, 1.66	1.82, 1.77	3.54, 3.48		−6.0

	chemical shift (ppm)						
	H4	H5	H8	H11	H12	H13	H14
Chr	**7.67**	**6.73**	**6.46**	**5.58**	**2.61, 2.20**	**3.51, 3.16**	**8.03**
	7.78	7.05	6.77	5.49	2.59, 2.26	3.55, 3.27	8.52

[a] Data for pyoverdin G4R−Ga(III) is in bold type; that for pyoverdin G4R free ligand is in normal type. Changes in chemical shift of >0.2 ppm are underlined.

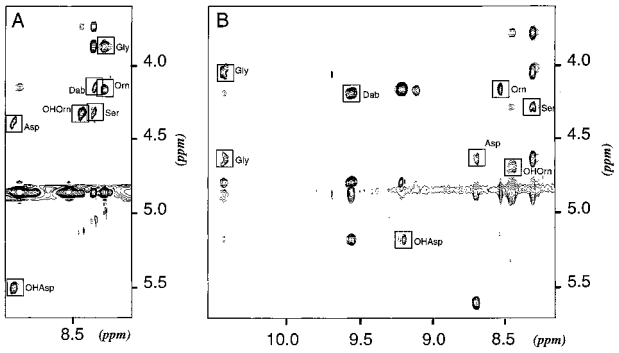

FIGURE 3: ROESY spectrum of pyoverdin G4R in H_2O/1% [$^2H_{10}$]-*tert*-butyl alcohol in the uncomplexed (A) and complexed (B) forms.

uncomplexed form the corresponding resonances covered only 1.0 ppm, is a clear indication of the structure of the peptide chain around the aromatic chromophore. Among the most notable changes in chemical shift are those of the Dab4 Hγ, Gly5 HN, and Gly5 Hα resonances, although changes of >0.2 ppm are also observed for the resonances of Chr H5 and H8, Asp1 Hα, OHAsp3 HN and Hβ, and OHOrn Hα (Table 1). In the complexed form, the Dab4 Hγ resonances are separated by 1.2 ppm as opposed to 0.1 ppm in the uncomplexed form, while the Gly5 Hα resonances, degenerate in the uncomplexed form, have chemical shifts that differ by 0.6 ppm in the complexed form. Also of note is the observation of Dab4 Hδ; the Nδ atom is not protonated under similar conditions in the free ligand.

Effects of Temperature. The assignments for uncomplexed pyoverdin G4R show no significant differences between 283 and 303 K, other than for the HN protons. Similarly, assignments at 303 K for complexed pyoverdin G4R−Ga(III) show no major changes from those at 283 K, for the chemical shifts of all ^{1}H nuclei other than the HN protons (data not shown). The pattern of cross-peaks in ROESY and NOESY spectra is unchanged, indicating that the tertiary structure of the complex is not perturbed greatly over this temperature range.

The chemical shifts of HN resonances are expected to decrease as the temperature is raised, as the hydrogen bonding environment is altered (*42*). "Random coil" values of temperature coefficients for the 20 natural amino acids (*43*) lie in a tight range between −7.0 and −8.4 ppb K^{-1}, except for those for aspartic acid (−6.4 ppb K^{-1}) and tyrosine (−9.3 ppb K^{-1}). Values that are smaller in magnitude than random coil values are sometimes taken as an indication of involvement in intramolecular hydrogen bonding and/or inaccessibility to solvent (*42*), but care must be taken in interpreting such results since they are also affected by conformational exchange processes.

For the pyoverdin G4R free ligand, only the temperature coefficient for the HN resonance of Gly5 is low (−4.5 ppb K^{-1}), all others lying close to random coil values (Table 1). This may indicate some small degree of structuring in solution. In contrast, the temperature coefficients of the HN resonances of complexed pyoverdin G4R−Ga(III) show greater variability (Table 1). While random coil values are not available for the nonstandard residues, the temperature coefficients for OHAsp3, Dab4, Gly5, Ser6, and OHOrn7 would appear to be low (−4.0 to −5.5 ppb K^{-1}), suggesting some protection from exchange with the solvent for these HN protons. In contrast, the values for Suc, Asp1, and Orn2 are high (−9.0 to −9.5 ppb K^{-1}). The value for Suc HN may be due to a greater lability resulting from its attachment to the aromatic system of the chromophore. Those for Asp1 and Orn2 may indicate conformational exchange.

Hydrogen Exchange. No HN resonances were observed in a spectrum recorded immediately after dissolution of uncomplexed pyoverdin G4R in D_2O. Two such resonances persisted, however, in the spectrum of pyoverdin G4R−Ga(III), when dissolved in D_2O. These resonances were assigned to the HN protons of OHAsp3 and Gly5.

Indications of Tertiary Structure. ROESY spectra of pyoverdin G4R free ligand (Figure 3) contain only intraresidual and sequential connectivities, indicating a largely

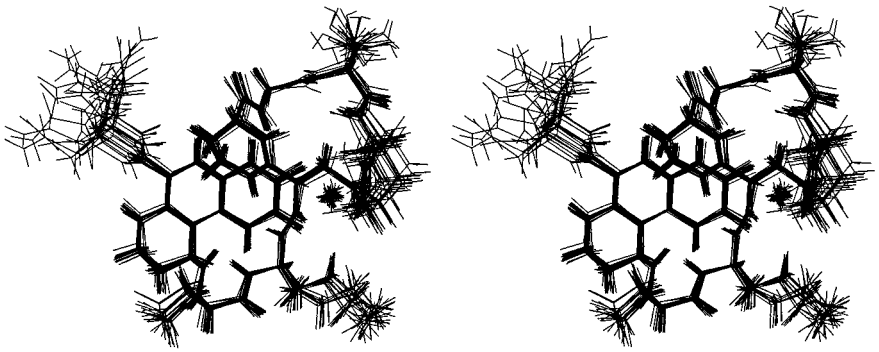

FIGURE 4: Superimposition of the set of 20 structures with the lowest overall energies of the pyoverdin G4R−Ga(III) complex.

Table 2: Statistics for the Family of 20 Calculated Structures of Pyoverdin G4R−Ga(III)[a]

E_{tot} (kcal mol^{-1})	48.18 (0.44)
E_{bonds} (kcal mol^{-1})	8.94 (0.20)
E_{angles} (kcal mol^{-1})	18.84 (0.33)
E_{impr} (kcal mol^{-1})	4.09 (0.40)
E_{vdW} (kcal mol^{-1})	0.60 (0.12)
$E_{distance-constraints}$ (kcal mol^{-1})	15.70 (0.53)
maximum violation (Å)	0.296 (0.023)
pairwise rmsd (Å)	0.186 (0.071)

[a] All values are means calculated over the set of 20 structures, except the pairwise rmsd which is the mean of all 190 pairwise fits. Fits were carried out using the carbon atoms of the two aromatic rings of the chromophore and the nitrogen and carbonyl carbon atoms of the peptidic backbone. The standard deviation is given in parentheses.

unstructured peptide chain. Coupling constants ($^3J_{HN-H\alpha}$) are all intermediate, characteristic of averaging between conformers.

The ROESY spectra of pyoverdins G4RA−Ga(III) and G4R−Ga(III) were essentially identical in all respects. This confirms that the replacement of OH by NH_2 on the succinate substituent of the chromophore has no effect on the tertiary structure of the pyoverdin−gallium complex. Since the former experiment did not require ^{15}N decoupling, it was used for quantification of cross-peak intensity. A number of distance constraints extracted from ROESY spectra (Figure 3) indicate tight packing of the peptide chain around the rigid chromophore. In particular, Chr H8 is close to Orn2 Hα, OHAsp3 HN, and Dab4 Hδ, while Chr H5, across the ring from Chr H8, forms cross-peaks with both Gly5 Hα resonances. In the complex, values of $^3J_{HN-H\alpha}$ were found to be large for Asp1, OHAsp3, and OHOrn7, suggesting that these residues may adopt β conformations ($\phi \sim -120°$ for L-amino acids).

Structure Calculations. The simulated annealing protocol, used to calculate three-dimensional structures consistent with the chemical structure of pyoverdin G4R−Ga(III) and with the distance constraints derived from ROESY spectra, produced a single set of structures of the complex. Of 100 runs, only two were rejected at the final stage because of poor covalent geometry. None of the structures had violations of the distance constraints greater than 0.5 Å. A set of 20 structures with the lowest overall energies is shown in Figure 4, and the breakdown of energetic terms is given in Table 2. Analysis of the distance violations in this set of final structures shows that the largest violations in each structure do not exceed 0.4 Å, and in all cases arise from intraresidue constraints on either the aliphatic cycle of Chr or the side chain of Orn2. Mean ϕ angles for the peptide chain all lie within 30° of expected values (determined from $^3J_{HN-H\alpha}$ coupling constants), with the exception of that of Asp1, for which the ϕ angle of around 53.0° is not expected to give rise to a coupling constant of >8 Hz. The average pairwise rmsd for the set of 20 structures is low, reflecting good convergence into a narrow energy minimum.

Tertiary Structure of Pyoverdin G4R−Ga(III). If the Ga(III) ion is considered as the center of the complex and the aromatic bicycle as forming a horizontal plane to its left (Figure 5), the first peptide bond drops almost vertically down off the chromophore. The chain sweeps around in a left-handed manner, placing Asp1 and Orn2, with their oppositely charged side chains disposed outward into solution, before arriving at a point below the metal ion, where OHAsp3 provides two coordinating oxygen atoms. The Hγ protons of Dab4 clearly lie in very different magnetic environments, due to the ring current effects of the aromatic rings, thus accounting for the large difference in their chemical shifts. The tetrahydropyrimidine ring serves to redirect the chain such that it then turns in a right-handed direction and upward to bring the ring of OHOrn7 into position for completing the coordination of the metal ion. As for the Dab4 Hγ protons, the Gly5 Hα protons experience differing magnetic environments; one lies close to Chr H5, almost in the plane of the aromatic rings, while the other is more distant and below the plane.

The Hδ proton of Dab4, labile in pyoverdin G4R free ligand, is directed inward toward the coordinating oxygen atoms, as are the HN protons of the neighboring residues, OHAsp3 and Gly5. These latter two HN protons were those observed to exchange slowly into D_2O, although inspection of the structure does not reveal hydrogen bonding partners for either proton.

The complex is a tightly defined, compact structure; only the succinamide group, ornithine side chain, and, to some extent, the ring of OHOrn7 are less well-defined. The metal ion is protected by the structure of the chromophore and the peptide chain, rigidified by the Dab64 residue in its center. Only between the side chains of OHAsp3 and OHOrn7 is the metal ion less shielded.

Alternative Configurations. Mean total energies for alternative configurations were between 1.33 and 6.1 times that of the structure presented above. This control excludes the possibility of having systematically found a false minimum in the calculations. The correct structure has a Δ absolute configuration, in accord with the circular dichroism spectrum.

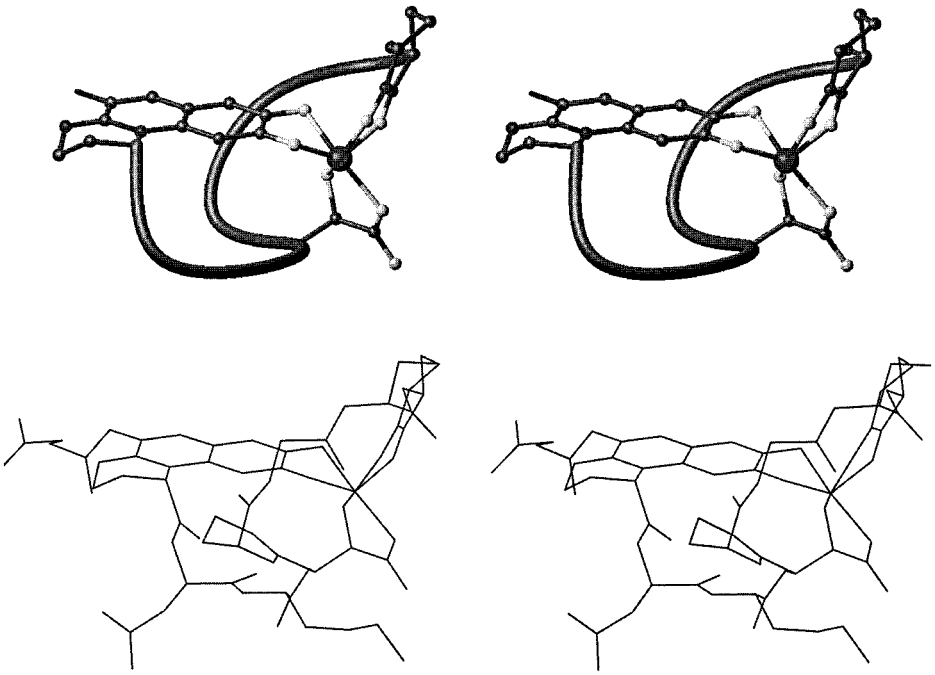

FIGURE 5: Stereoviews of ball-and-stick and line representations of the tertiary structure of the pyoverdin G4R−Ga(III) complex. Only the heavy atoms of the residues in the vicinity of the chelation center are detailed: the chromophore, β-hydroxyaspartic acid, and *cyclo*-N^{δ}-hydroxyornithine. The main peptide chain is represented by a ribbon going through the Cα positions. The succinate residue on C3 of the chromophore is not represented in the ball-and-stick model. In the line representation, all the heavy atoms are shown.

DISCUSSION

The requirements of *Pseudomonas* bacteria for iron are fulfilled by a remarkable mechanism, involving the biosynthesis of small but intricate molecules (pyoverdins) able to complex Fe(III), and systems for secretion, recovery, interiorization, and reduction. The most striking feature of the pyoverdins is their high affinity for Fe(III). For pyoverdin G4R in particular, this is achieved in a most economical manner, in terms of molecular size.

The role and the nature of the amino acids which do not participate in the coordination of iron(III) and the steric requirements for the interaction of the complexed pyoverdins with the outer-membrane receptors are not yet clear. The iron uptake process takes place in two steps: recognition of the complex by the receptor, very strongly influenced by the nature of the three bidentate groups (cathechol and α-hydroxyaspartic and hydroxamic acids) and their location in the peptide chain, and then transport into the cell (*44*), dependent on the nature of the other residues. In the case of *Neurospora crassa*, the cyclic nature of the peptide is not required for the binding of the iron coordination region of the siderophore complex to the receptor, but is necessary for the subsequent transport (*45*).

Concerning pyoverdins, results from cross-feeding experiments for seven fluorescent *Pseudomonas* strains have shown that the pyoverdin-mediated iron transport systems are strictly strain-specific for a majority of them (*46*, *47*). Although the pyoverdins produced by different strains are very similar in their overall structure, small differences in the nature and location in the peptide chain of one or two amino acids, which are not involved in the coordination of the metal, are important enough to determine the specificity. However, in very few cases, this specificity seems to be less strict, as for pyoverdins from *Pseudomonas aeruginosa* ATCC 15692, *Pseudomonas fluorescens* ATCC 13525, and *Pseudomonas chlororaphis* ATCC 9446. These strains produce pyoverdins which are structurally very closely related. *P. fluorescens* ATCC 13525 and *P. chlororaphis* ATCC 9446 produce mixtures of pyoverdins with identical structures (*14*). *P. aeruginosa* ATCC 15692 has a very closely related structure (*18*, *19*), with identical chelating bidentate groups, minor alterations to the peptide sequence, and a change in stereochemistry of one of the hydroxyornithines.

Consequently, the structural requirements for the interaction of each of these pyoverdins with their respective receptors are sufficient for the recognition process, and these siderophores are interchangeable. To date, this is a unique case.

The chromophore represents the common feature between *Pseudomonas* pyoverdins, probably indicating a biosynthetic pathway conserved through evolution. The variability of the acid or amide substituent on C3 of the chromophore suggests that it has little importance beyond protection from hydrolysis of an aromatic free amine group to a hydroxyl group and plays no role in binding of the complexed pyoverdin to its receptor. The peptide chain that provides the two additional bidentate ligands to complex Fe(III) is unique to each species of *Pseudomonas*, indicating a specialization by each bacteria of its pyoverdin. This chain must contain the residues required to achieve coordination of the metal ion and to confer specificity, on complexation, for its own receptor.

Comparison of the three known pyoverdin structures (*22*, *23*) (Figure 6) shows that the coordination is not achieved in the same manner in all pyoverdins; while pseudobactin B10−Fe(III) and pyoverdin GMII−Ga(III) have Λ configurations about the metal ion, pyoverdin G4R−Ga(III) has a Δ configuration. Furthermore, the manners in which the two latter molecules complex their metal ion are Δ and Λ of the same isomer.

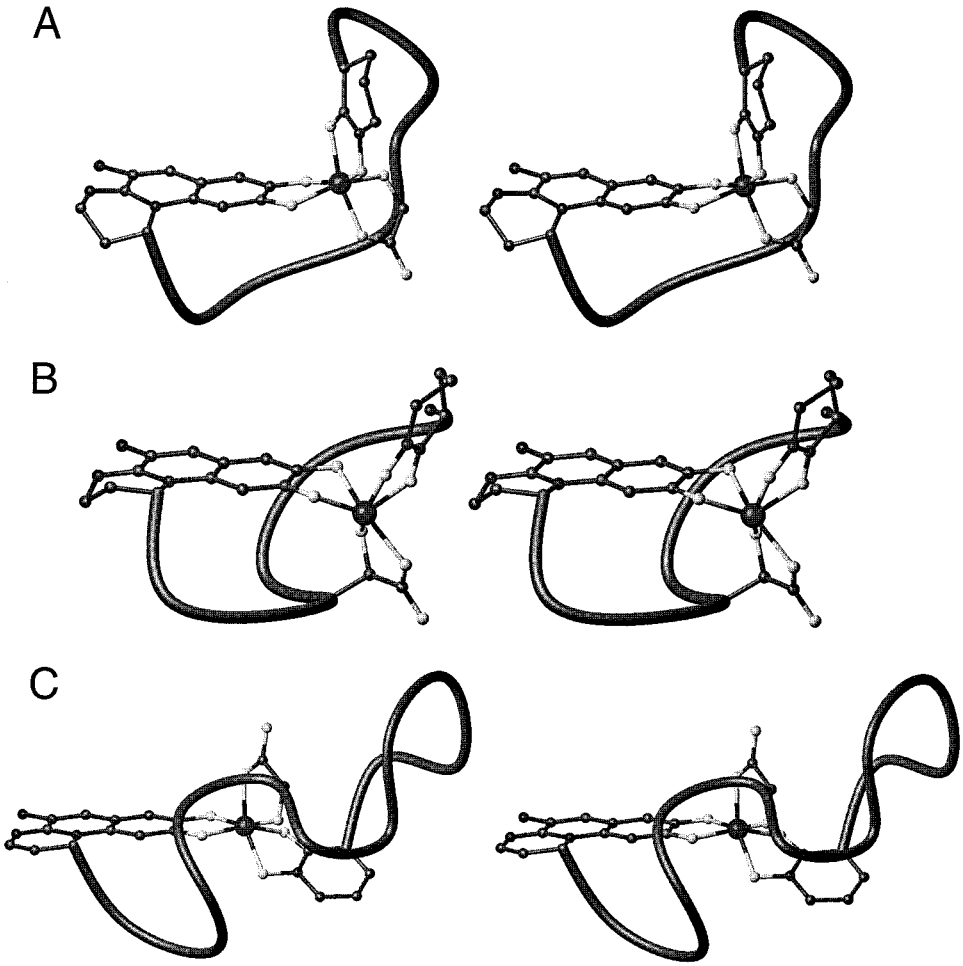

FIGURE 6: Comparison of the three known pyoverdin structures: stereoviews of ferric pseudobactin (A) (*22*), pyoverdin G4R−Ga(III) complex (B), and pyoverdin GMII−Ga(III) complex (C) (23). The representations of the ball-and-stick views are the same as those in Figure 5.

The pyoverdin G4R peptide chain is short, with a minimal number of residues between those that complex the metal ion, and the three residues between OHAsp3 and OHOrn7 structured by the tetrahydropyrimidine ring of Dab4. Pseudobactin B10 also contains three residues between its two peptidic coordinating residues, but these form a more flexible sequence L-Ala-D-*allo*-Thr-L-Ala. Pyoverdin GM-II, on the other hand, has longer, more flexible segments, D-Ala-D-Lys-Gly-Gly, between the chromophore and the hydroxyaspartic acid, and D-Gln-D-Ser-L-Ala-D-Ala-D-Ala-L-Ala, between the two coordinating residues, that appear to have little to do with metal binding. If this latter sequence is involved in receptor binding, then what features of the pyoverdin G4R−Ga(III) determine its binding to its receptor? OHAsp3 and OHOrn7 are involved in metal coordination; Dab4 and Gly5 have an important structural role in reversing the direction of the peptide chain, and only Asp1, Orn2, and Ser6 remain as possible residues for determining receptor binding. It may rather be, however, that it is the fold around the octahedrally coordinated metal ion that is recognized, i.e., a surface formed by the ring of OHOrn7 and parts of the side chains of Orn2, OHAsp3, and Ser6. The corresponding surface for pseudobactin B10−Fe(III) would be formed by the C-terminal *cyclo*-hydroxyornithine ring and the sequence L-Ala-D-*allo*-Thr-L-Ala.

The isolation and characterization of pyoverdins G4R and G4RA and the preparation of ^{15}N-labeled samples (*1*) have enabled detailed structural and dynamic characterization of these molecules in their uncomplexed and complexed states. The dynamic behavior of pyoverdin G4R, as free ligand and complex, will be discussed elsewhere, in light of the three-dimensional structure presented here.

ACKNOWLEDGMENT

We thank the members of our respective groups for useful discussions, Dr. Franc Pattus for allowing access to the CD spectrometer and assistance in its use, and Dr. Danielle Promé for measuring the mass spectum of the gallium(III) complexes.

REFERENCES

1. Salah El Din, A. L. M., Kyslìk, P., Stephan, D., and Abdallah, M. A. (1997) *Tetrahedron 53*, 12539−12552.
2. Dolphin, D. (1982) in *The Biological Chemistry of Iron* (Dunford, H. B., Dolphin, D., Raymond, K. N., and Sieker, L., Eds.) pp 283−294, Dordrecht, Riedel, Germany.
3. Stryer, L. (1988) in *Biochemistry*, 3rd ed., pp 397−426, W. H. Freeman & Co. Publishers, New York.
4. Neilands, J. B., Konopka, K., Schwyn, B., Coy, M., Francis, R. T., Paw, B. H., and Bagg, A. (1987) in *Iron Transport in Microbes, Plants and Animals* (Winkelmann, G., Van der Helm, D., and Neilands, J. B., Eds.) pp 3−33, VCH Verlaggesellschaft, Weinheim, Germany.
5. Lankford, C. E. (1973) *Crit. Rev. Microbiol. 2*, 273−331.
6. Neilands, J. B. (1982) *Annu. Rev. Microbiol. 36*, 285−309.

7. Griffiths, E. (1990) *J. Biosci. 15*, 173−177.
8. Wayne, R., and Neilands, J. B. (1975) *J. Bacteriol. 121*, 447−452.
9. Hancock, R. E. W., and Braun, V. (1976) *J. Bacteriol. 125*, 409−415.
10. Hollifield, W. C., Jr., and Neilands, J. B. (1978) *Biochemistry 17*, 1922−1928.
11. Royt, P. W. (1990) *Biol. Met. 3*, 28−33.
12. Covès, J., and Fontecave, M. (1993) *Eur. J. Biochem. 211*, 635−641.
13. Abdallah, M. A. (1991) in *Handbook of Microbial Iron Chelates* (Winkelmann, G., Ed.) pp 139−153, CRC Press Inc., Boca Raton, FL.
14. Linget, C., Azadi, P., MacLeod, J. K., Dell, A., and Abdallah, M. A. (1992) *Tetrahedron Lett. 33*, 1737−1740.
15. Demange, P., Wendenbaum, S., Linget, C., Bateman, A., MacLeod, J. K., Dell, A., Albrecht, A. M., and Abdallah, M. A. (1989) in *Second Forum on Peptides* (Aubry, A., Marraud, M., and Vitoux, B., Eds.) Vol. 174, pp 95−98, INSERM, J. Libbey Eurotext Ltd.
16. Albrecht-Gary, A. M., Blanc, S., Rochel, N., Ocaktan, A. Z., and Abdallah, M. A. (1994) *Inorg. Chem. 33*, 6391−6402.
17. Poppe, K., Taraz, K., and Budzikiewicz, H. (1987) *Tetrahedron 43*, 2261−2272.
18. Briskot, G., Taraz, K., and Budzikiewicz, H. (1989) *Liebigs Ann. Chem. 4*, 375−384.
19. Demange, P., Wendenbaum, S., Linget, C., Mertz, C., Cung, M. T., Dell, A., and Abdallah, M. A. (1990) *Biol. Met. 3*, 155−170.
20. Wong-Lun-Sang, S., Bernardini, J. J., Hennard, C., Kyslik, P., Dell, A., and Abdallah, M. A. (1996) *Tetrahedron Lett. 37*, 3329−3332.
21. Yang, C. C., and Leong, J. (1984) *Biochemistry 23*, 3534−3540.
22. Teintze, M., Hossain, M. B., Barnes, C. L., Leong, J., and Van der Helm, D. (1981) *Biochemistry 20*, 6446−6457.
23. Mohn, G., Koehl, P., Budzikiewicz, H., and Lefèvre, J.-F. (1994) *Biochemistry 33*, 2843−2851.
24. Demange, P., Bateman, A., Dell, A., and Abdallah, M. A. (1988) *Biochemistry 27*, 2745−2752.
25. Marion, D., and Wüthrich, K. (1983) *Biochem. Biophys. Res. Commun. 113*, 967−974.
26. Aue, W. P., Bartholdi, E., and Ernst, R. R. (1976) *J. Chem. Phys. 64*, 2229−2246.
27. Piantini, U., Sørensen, O. W., and Ernst, R. R. (1982) *J. Am. Chem. Soc. 104*, 6800−6801.
28. Braunschweiler, L., and Ernst, R. R. (1983) *J. Magn. Reson. 53*, 521−528.
29. Bax, A., and Davis, D. G. (1985) *J. Magn. Reson. 65*, 355−360.
30. Jeener, J., Meier, B. H., Bachmann, P., and Ernst, R. R. (1979) *J. Chem. Phys. 71*, 4546−4553.
31. Bothner-By, A. A., Stephens, R. L., Lee, J., Warren, C. D., and Jeanholz, R. W. (1984) *J. Am. Chem. Soc. 106*, 811−813.
32. Piotto, M., Saudek, V., and Sklenár, V. (1992) *J. Biomol. NMR 2*, 661−665.
33. Shaka, A. J., Barker, P. B., and Freeman, R. (1985) *J. Magn. Reson. 64*, 547−552.
34. Karplus, M. (1959) *J. Chem. Phys. 30*, 11−15.
35. Pardi, A., Billeter, M., and Wüthrich, K. (1984) *J. Mol. Biol. 180*, 741−751.
36. Wagner, G., Braun, W., Havel, T. F., Schaumann, T., Go, N., and Wüthrich, K. (1987) *J. Mol. Biol. 196*, 611−638.
37. Brünger, A. T. (1992) *X-PLOR Software Manual*, version 3.1, Yale University Press, New Haven, CT.
38. Wüthrich, K., Billeter, M., and Braun, W. (1983) *J. Mol. Biol. 169*, 949−961.
39. Hossain, M. B., Eng-Wilmot, D. L., Loghry, R. A., and Van der Helm, D. (1980) *J. Am. Chem. Soc. 102*, 5766−5773.
40. Demange, P., Bateman, A., Mertz, C., Dell, A., Piémont, Y., and Abdallah, M. A. (1990) *Biochemistry 29*, 11041−11051.
41. Wüthrich, K. (1986) *NMR of Proteins and Nucleic Acids*, Wiley, New York.
42. Baxter, N. J., and Williamson, M. P. (1997) *J. Biomol. NMR 9*, 359−369.
43. Merutka, G., Dyson, H. J., and Wright, P. E. (1995) *J. Biomol. NMR 5*, 14−24.
44. Winkelmann, G., and Huschka, H.-G. (1987) in *Iron Transport in Microbes, Plants and Animals* (Winkelmann, G., Van der Helm, D., and Neilands, J. B., Eds.) pp 317−336, VCH Verlaggesellschaft, Weinheim, Germany.
45. Huschka, H.-G., Naegeli, H. U., Leuenberger-Ryf, H., Keller-Schierlein, W., and Winkelmann, G. (1985) *J. Bacteriol. 162*, 715−721.
46. Hohnadel, D., and Meyer, J.-M. (1988) *J. Bacteriol. 170*, 4865−4873.
47. Cornelis, P., Hohnadel, D., and Meyer, J.-M. (1989) *Infect. Immun. 57*, 3491−3497.

BI981194M